Journal of Thermal Analysis and Calorimetry, Vol. 64 (2001) 331–339

SIMULTANEOUS OBSERVATION OF HYPERFINE MULTISTAGE TRANSITIONS OF $BaTiO_3$ WITH THERMAL ANALYSIS AND THERMAL EXPANSION

K. Tozaki[1], *R. Masuda*[1], *S. Matsuda*[1], *C. Tokitomo*[1], *H. Hayashi*[1], *H. Inaba*[1], *Y. Yoshimura*[2] *and T. Kimura*[3]

[1]Faculty of Education, Chiba University, Inage, Chiba 263-8522, Japan
[2]Department of Physics, Faculty of Science and Engineering, Ritsumeikan University, Kusatsu, Shiga 525-8577, Japan
[3]Department of Industrial Chemistry, Faculty of Engineering, Tokyo Metropolitan University, Minami-osawa, Hachioji, Tokyo 192-0397, Japan

Abstract

A new method to measure heat flux and thermal expansion simultaneously with a temperature resolution of milli-Kelvin is presented to observe the multistage transitions. At least six thermal anomalies are observed between 402 and 403 K in $BaTiO_3$ simultaneously in heat flux and thermal expansion in the cooling process. The correspondence of the anomalies observed in the two physical properties is excellent.

Keywords: $BaTiO_3$, heat flux, multiple phase transition, thermal anomaly, thermal expansion

Introduction

There have been a number of solid–solid phase transitions found in various kinds of materials. They appear in most cases as a single-stage transition occurring at a definite temperature. In some cases, however, two or more transitions occur successively at a very small temperature interval. To what extent these multistage transitions can be detected depends on the temperature resolution determined by the temperature stability in a sample cell for measurements. We have developed a milli-Kelvin stabilized thermal apparatus for that purpose [1, 2]. It is also desirable to develop a method to detect the multistage transitions simultaneously observing multiple thermodynamic properties such as heat capacity and thermal expansion.

In this paper, we present a new method to measure heat flux and thermal expansion simultaneously with a temperature resolution of milli-Kelvin to observe the multistage transitions. The central part of the apparatus is made of a special metal cell on a metal block whose temperature is controlled with a precision better than 50 μK. A solid sample is sandwiched by a metal plate and a thermomodule. Heat flux is detected by the thermomodule and thermal expansion is detected by observing the change of capacitance due to the change of the sample length.

1418–2874/2001/ $ 5.00

Akadémiai Kiadó, Budapest
Kluwer Academic Publishers, Dordrecht

Experimental

The apparatus for the simultaneous measurement

The central part of the apparatus for the simultaneous measurements of heat flux and thermal expansion is schematically shown in Fig. 1. The sample cell is composed of a

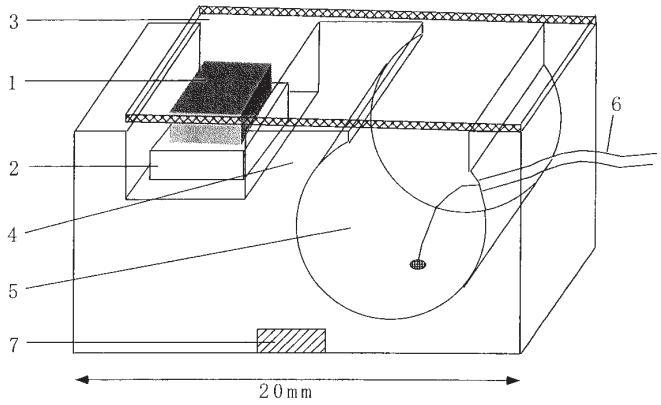

Fig. 1 Schematic drawing of the sample cell.
1 – sample, 2 – semiconducting thermoelectric module (TM1), 3 – metal plate, 4 – metal block (Cu), 5 – cylindrical bore of the metallic block, 6 – coaxial cable, 7 – Pt temperature sensor (TS1)

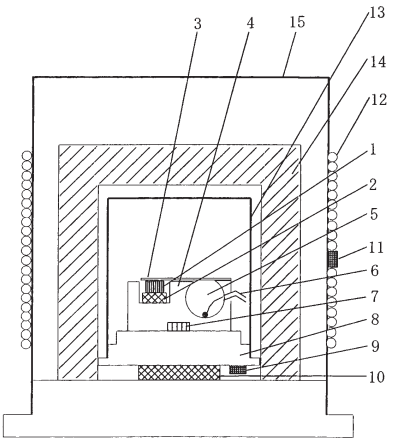

Fig. 2 Schematic drawing of the apparatus.
1 – sample, 2 – semiconducting thermoelectric module (TM1), 3 – metal plate, 4 – metal block (Cu), 5 – cylindrical bore of the metallic block, 6 – coaxial cable, 7 – Pt temperature sensor (TS1), 8 – base metal block (Cu), 9 – Pt temperature sensor (TS2), 10 – thermoelectric module (TM2), 11 – Pt temperature sensor (TS3), 12 – cylindrical heater, 13 – metal shield, 14 – ceramic thermal shield, 15 – metal shield

sample (1), a thermoelectric module (2) and a metallic plate of phosphor bronze (3), which are in a well of a metallic block (4). The sample (1) is sandwiched by the thermoelectric module (2) and the metallic plate (3). The whole apparatus is schematically shown in Fig. 2. The measurement can be made in either direction of heating or cooling in this apparatus. The temperature of the metal shield (15) was controlled by a cylindrical heater (12) using a Pt temperature sensor, TS3 (11). The temperature of the copper block (8) was controlled using a Pt temperature sensor, TS2 (9) and a semiconducting thermoelectric module, TM2 (10), working as a heat pump by Peltier effect. TM2 can pump heat in either direction to heat or cool the copper block by changing the magnitude and the direction of the current through it. An insulating thermal shield (14) is between the metal shields (13) and (15) in order to minimize the fluctuation of the temperature of metal block (8). The temperature of the metal block (4) made of copper, was occasionally monitored by a Pt temperature sensor, TS1 (7), but it was not used in the usual measurement due to the Joule heating effect, which gives thermal inhomogeneity around the sample.

The measurement of heat flux

For the measurement of heat flux, the thermoelectric module (2) , TM1, was glued on the well of the metallic block (4). It is composed of many semiconducting thermoelectric elements connected in series and generates electromotive force by the Seebeck effect when there is a temperature difference between the two substrates of the thermomodule due to endothermic or exothermic change in the sample. Since the calibration of the heat flux of this apparatus is difficult due to the heat leak from the metal plate (3) contacting the sample, the calibration was conducted by using the differential scanning calorimeter of our laboratory [1, 2] using the same thermoelectric module, TM1. Heat flux was measured by the DSC using a sapphire sample and the reference heat capacity data of the sapphire in the calibration. Using the same calibration factor as DSC, the magnitude of the heat flux for this apparatus was given.

The measurement of thermal expansion

For the measurement of thermal expansion, LC resonance circuit was formed using the metal block (4) with a bore and a narrow air-gap. The cylindrical bore (5) of the metallic block (4) is for obtaining a proper inductance L of the LC resonance circuit. The tip of the coaxial cable (6) was soldered in the cylindrical bore (5) for the network measurement of the circuit. The capacitance C of the circuit was determined by the air gap less than 0.1 mm between the central part of the metallic block (4) and the metallic plate (3). When the sample is thermally expanded, the metallic plate (3) is pushed to upper side and then the air gap increases. The increase of the air gap changes the resonant frequency f, which was about 1 GHz in this arrangement and was measured by a network analyzer (HP8753E) through the cable (6). The relation between the resonant frequency f and the magnitude of L and C in the circuit is given as:

$$f=1/\{2\pi(LC)^{1/2}\} \quad (1)$$

When the area in which the central part of the metallic block (4) and the metallic plate (3) face each other is written as S, the capacitance component C is given as:

$$C=\varepsilon S/h \quad (2)$$

where ε is the dielectric constant of air and h is the length of the air gap. The thermal expansion of the apparatus, Δh, is represented by the sum of Δh_1 and Δh_2, where Δh_1 is the thermal expansion of the sample and Δh_2 is composed of the contribution of the thermomodule and air gap. Then, Δh can be shown as:

$$\Delta h=\Delta h_1+\Delta h_2=\{\varepsilon S/(4\pi^2 L)\}(2f\Delta f+\Delta f^2) \quad (3)$$

Since Δf is far smaller than f in usual conditions, Δf^2 is negligibly small compared with $2f\Delta f$, Δh becomes as:

$$\Delta h=\Delta f f\varepsilon S/(2\pi^2 L) \quad (4)$$

Therefore, Δh is proportional to Δf and the proportional coefficient, $f\varepsilon S/(2\pi^2 L)$, can be determined by thermal expansion experiments using known samples.

Sample for the measurement

A single crystal of $BaTiO_3$ was prepared by a top-seeded solution growth technique [3]. The single crystals were grown from the melt of the mixture of TiO_2/BaO=65/35 in molar ratio. The sources of TiO_2 and $BaCO_3$ were 99.99 and 99.999% purity powders, respectively. The as-grown crystals with the dimension of about 20×20×15 mm^3 were cut. One of the faces of the cut plane was (100) plane and the measurement of heat flux and thermal expansion was conducted in the direction perpendicular to the (100) plane.

Results and discussion

Temperature stability of the apparatus

The temperature of the sample cell was controlled twofold by a rough control using the heater (11) and a precise control using the thermomodule, TM2. In order to check the temperature stability of the apparatus, the variation of the temperatures at about 308 K was measured and is shown in Fig. 3. As seen in Fig. 3, the temperature detected with TS3, was controlled to be within ±0.6 mK, and that by TS2, whose fluctuation of temperature becomes small due to the dumping effect of the insulating thermal shield and the metal blocks, was controlled to be within ±50 μK. The temperature of the metal block (4) of the sample cell, $T_{S,1}$, was not usually measured due to the Joule heating effect of Pt temperature sensor during the measurement, but was nearly equal to $T_{S,2}$ within an error of 1 mK in the usual measuring conditions. The temperature detected with TS2 was then regarded as the temperature of the sample. The baseline of the heat flux is also shown in Fig. 3, where the fluctuation of the baseline is

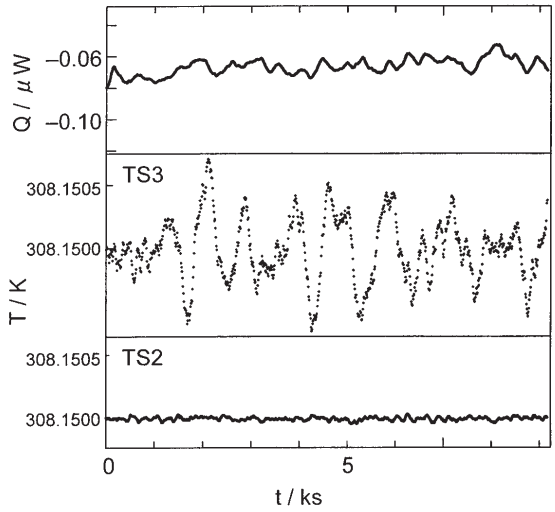

Fig. 3 Temperature variation of $T_{S,2}$ and $T_{S,3}$ and stability of the baseline for the heat flux measurement

within ±15 nW. Such a stable baseline is considered to be achieved by a very stable temperature at the metal block of the sample cell, $T_{S,1}$, which is considered to be several times more stable than $T_{S,2}$.

Heat flux and thermal expansion of $BaTiO_3$ in the heating process

Before conducting the simultaneous measurements of heat flux and thermal expansion, the thermal expansion of a single crystal $BaTiO_3$ along <100> direction was measured by using a conventional dilatometer of the push-rod type at a heating rate of

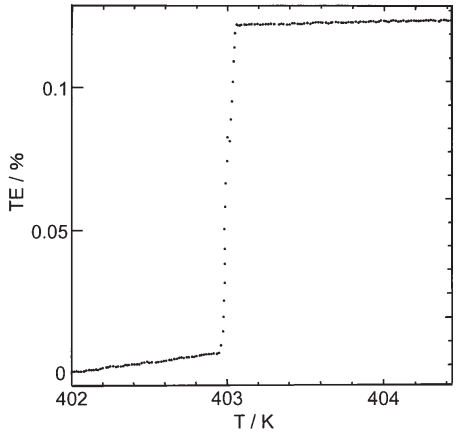

Fig. 4 Thermal expansion of a single crystal $BaTiO_3$ along <100> direction at a heating rate of 0.1 K min^{-1} using a push-rod type dilatometer

0.1 K min^{-1} and is shown in Fig. 4. As seen in Fig. 4, a clear thermal expansion anomaly is observed at about 404 K. This anomaly is considered to be due to the ferroelectric-paraelectric transition. This result can be used as a reference value to determine the proportional factor in Eq. (4) in the simultaneous measurement. The simultaneous measurement of heat flux and thermal expansion was conducted along <100> direction (perpendicular to the (100) face) of the single crystal $BaTiO_3$ with the size of 1.3×3.3×5.5 mm^3 using the apparatus shown in Fig. 2. The results of the simultaneous measurement at a heating rate of 10 μK s^{-1} are shown in Fig. 5. The right ordinate of the thermal expansion in Fig. 5 shows the resonant frequency *f* in Eq. (4) ranging from 973 to 976 MHz. It is converted to the thermal expansion in the unit of %, which is shown in the left ordinate in Fig. 5, assuming that the jump width of the thermal expansion around 403 K shown in Fig. 4 is the same as that in Fig. 5.

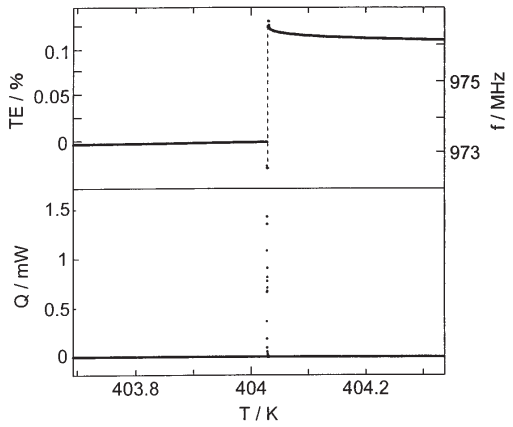

Fig. 5 Thermal expansion and heat flux measured simultaneously at a heating rate of 10 μK s^{-1} for a single crystal $BaTiO_3$ along <100> direction

It is seen in Fig. 5 that a single sharp endothermic anomaly and a sharp thermal expansion anomaly at about 404 K. This behavior is characteristic to the first-order phase transition being consistent with previous studies [3, 4].

Successive hyperfine phase transitions of $BaTiO_3$ in the cooling process

In the case of the cooling process, however, heat flux and thermal expansion for $BaTiO_3$ measured at a cooling rate of 0.2 mK s^{-1} show quite different behaviors from the heating process, as shown in Fig. 6. We can see at least six thermal anomalies between 402 and 403 K both in heat flux and thermal expansion. The heat flux and thermal expansion at a slower cooling rate of 10 μK s^{-1} are shown in Fig. 7, where anomalies become separate and sharper.

The heat flux (heat capacity) anomalies shows many straight lines and the thermal expansion anomalies shows discontinuous points in the thermal expansion curve.

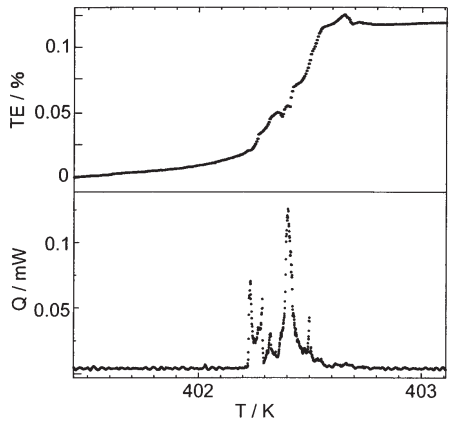

Fig. 6 Thermal expansion and heat flux measured simultaneously at a cooling rate of 0.2 mK s^{-1} for a single crystal $BaTiO_3$ along <100> direction

The reason for this different behaviors of the two physical properties comes from the fact that heat capacity is a second derivative of Gibbs energy, while that thermal expansion is a first derivative of Gibbs energy. Therefore, the derivative of the thermal expansion curve in Fig. 7, namely the thermal expansion coefficient is taken and is shown in Fig. 8. As seen in Fig. 8, most of the anomalies in heat flux and thermal expansion coefficient correspond but some show different behaviors. They are classified into three groups.

First one is the corresponding thermal expansion anomaly and heat flux anomaly, such that at 402.73 K. Second one is the combination of thermal expansion and contraction and the corresponding heat flux anomaly, such that at 402.48 and 402.98 K. Third one is the heat flux anomaly and no anomaly in thermal expansion, such that at 402.83 K. These behaviors show the character of each anomaly and the detailed analysis of them is awaited to clarify the mechanism of the hyperfine multistage phase transitions. Thus there is an advantage to measure two physical properties simultaneously in order to study the hyperfine multistage phase transitions.

The anomaly at the heating process appears at 404.03 K, while the main anomaly in the cooling process appears at about 402.73 K. Both processes accompany about 0.12% change of thermal expansion. These facts indicate that the main anomaly in the cooling process at 402.73 K is due to a long range ordering of ferroelectric domains to form the ferroelectric phase. In the heating process, the nucleation of the cubic phase is difficult due to a large energy to form interface from the mother tetragonal phase until 404.03 K forming the single anomaly, where thermal energy is enough to transform the tetragonal phase into the cubic phase. In the cooling process, the nucleation of the tetragonal phase can appear stepwisely in a short range from the mother cubic phase resulting in anomalies at 403.22, 402.98, 402.83 and 402.76 K as seen in Fig. 7. The main anomaly in the cooling process is composed of two steps at 402.73 and 402.72 K. The anomaly at 402.48 K in the cooling process may show that another mode of displacement of atoms may occur in the ferroelectric phase.

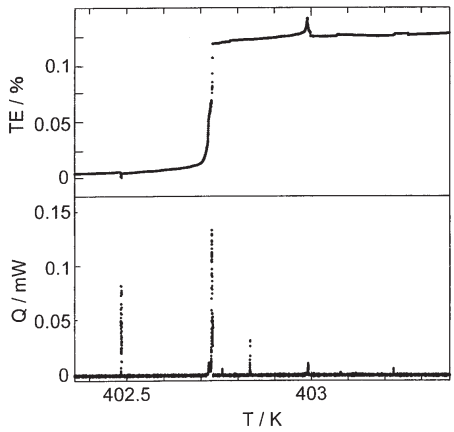

Fig. 7 Thermal expansion and heat flux measured simultaneously at a cooling rate of 10 μK s^{-1} for a single crystal $BaTiO_3$ along <100> direction

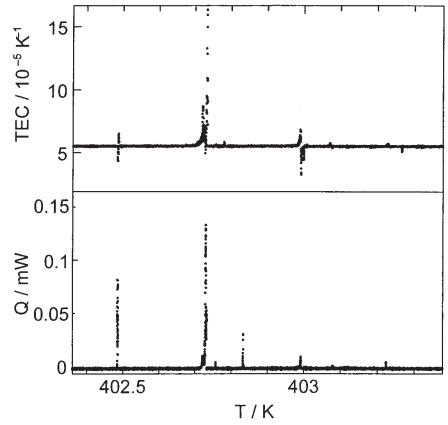

Fig. 8 Thermal expansion coefficient and heat flux measured simultaneously at a cooling rate of 10 μK s^{-1} for a single crystal $BaTiO_3$ along <100> direction

Similar successive thermal anomalies have been observed in $CsPbCl_3$ [1], which has the same perovskite structure as $BaTiO_3$. The mechanism of such successive thermal anomalies in $CsPbCl_3$ has been considered as due to the condensation of the vibration mode of $PbCl_6$ octahedra and the phonon instabilities taking place successively at M, R, X points in the cubic Brilloun zone [1]. Although the hysteresis in the thermal anomalies between the heating and cooling process in $CsPbCl_3$ is rather small, that in $BaTiO_3$ is quite large. The similarity and the difference in the thermal anomalies between the two compounds are quite interesting and further studies are necessary to clarify them.

We would like to thank Mr. O. Nakao of Materials Research Laboratory of Fujikura Ltd., for providing the single crystal of $BaTiO_3$.

References

1 K. Tozaki, C. Ishii, A. Kojima, Y. Yoshimura, O. Izuhara, K. Yamada, H. Iwasaki, Y. Noda and J. Harada, Phys. Lett. A, 263 (1999) 203.
2 A. Kojima, Y. Yoshimura, H. Iwasaki and K. Tozaki, Ferroelectrics, 237 (2000) 119.
3 A. Kurosaka, K. Tomomatsu, O. Nakao, S. Ajimura, H. Tominaga and H. Osanai, Sozaibusseigakuzasshi, 5 (1992) 74.
4 I. Hatta, Thermochim. Acta, 304/305 (1997) 27.
5 I. Hatta and A. Ikushima, J. Phys. Soc. Jpn., 41 (1976) 558.